SIZE/MASS-FREQUENCY DISTRIBUTIONS OF DUST-SIZE DEBRIS FROM THE IMPACT DISRUPTION OF CHONDRITIC METEORITES. D. D. Durda[1], G. J. Flynn[2], L. E. Sandel[3], and M. M. Strait[3]. [1]Southwest Research Institute, 1050 Walnut Street Suite 400 Boulder CO 80302 durda@boulder.swri.edu, [2] SUNY-Plattsburgh Plattsburgh NY 12901, [3]Alma College Alma MI 48801.

Introduction: In order to understand the collisional evolution of asteroids and interplanetary dust and to accurately model the infrared signature of small particles in our own Solar System and in other young planetary systems, we must address the fundamental problem of better understanding dust production from primary impact disruption events covering a wide range of sizes. At present, however, we understand well the size-frequency distributions (SFDs) for collision fragments within only a couple orders of magnitude of the size scale of the original target body; for impact disruption events at all size scales we still know next to nothing (and in many cases identically nothing) about the primary production of fragments many orders of magnitude smaller than the original target body size. Thus, existing modeling results in these areas have tremendous uncertainties.

Laboratory-scale impact experiments can provide direct knowledge of the SFDs of dust-size debris produced directly from the impact disruption of ~5-cm scale meteorite targets, roughly the size scale of the immediate parent bodies of zodiacal dust particles. Here, we report results of a set of impact disruption experiments involving chondritic meteorite samples, conducted at the NASA Ames Vertical Gun Range (AVGR). Preliminary results from some of these experiments were reported previously in [1].

Impact Experiments: Chondrite meteorites were impacted by small aluminum projectiles at speeds of about 5 km/s in order to examine the production of dust particles and the mechanics of fracture of real meteoritic materials under the impact regimes that presently exist in the main asteroid belt. The ~5 cm-scale targets were each suspended at the center of the AVGR impact chamber and surrounded with (typically) four passive dust 'detectors' consisting of thin aluminum foils (~7- and 13-μm thick, mounted in 35mm slide mounts, and 51-μm thick, taped across larger cutouts in the detector foam core backing) and rectangular blocks of aerogel (with dimensions of ~2×2×3 cm). Figure 1 shows one of the detectors in detail and in place in the impact chamber near one of the meteorite targets. The foils were thin enough to allow high-speed particles to penetrate, providing a size distribution of ejecta; particles captured intact in the aerogel were analyzed *in situ* for chemical composition [2,3]. Large fragments were collected from the chamber and weighed. The impacts were recorded by 500 fps video.

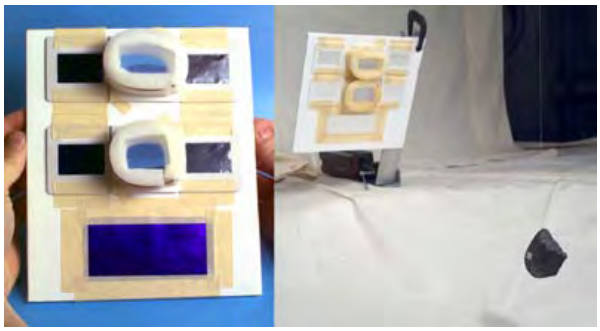

Figure 1. Passive particle detectors used in AVGR impact experiments to capture and measure the properties of dust-size debris. (Left) Detail showing the arrangement of foils and aerogel in a typical detector layout. ~7-, 13-, and 51-μm thick foils are set along the top, middle, and bottom rows, respectively, with blocks of aerogel set in foam holders between the foils. (Right) Typical deployment of a detector near a meteorite target within the AVGR impact chamber.

Foil Hole Data: The techniques for obtaining foil hole diameters are described in detail in [4]. To cover the entire area of a particular foil (equal to the window size of a standard 35mm slide mount), the foil was scanned with a Canon Canoscan FS 4000US slide scanner at 4000 dpi. The resulting 4000×5888 pixel images have a resolution of ~6.3 μm/pixel. Figure 2 shows an example of a slide foil image scanned previously with a lower resolution, 2700 dpi scanner. Smaller, sample areas of some foils were surveyed with a microscope/video setup at a resolution of ~1.6 μm/pixel. The holes generally display two distinct morphologies: some appear to represent comparatively low-speed ejecta and tend to lie at the bottom of stretched impact depressions in the foil, while others clearly resulted from high-speed particles, being cleanly punched and displaying surrounding, raised rims.

The hole sizes from the resulting scanner images were determined by analysis with the software package ImageJ from NIH, which was used to determine the area of each hole and to convert that area to the diameter of a circular hole having the same area. The foil hole diameter data were converted to impacting particle diameters using the calibration data of [5], presented in their Figure 14. We assume here a particle

speed of 2 km/s sec, the slowest of the calibrated impact speeds. To generate a cumulative particle mass-frequency distribution from the foil penetration data in order to combine with and extend the mass-frequency data from larger, weighed fragments, it was then necessary to convert the particle diameter to particle mass. We assumed particle densities of 2 gm/cm^3 and 3 gm/cm^3. Two sets of data points are shown for the foil data, one for each of the two density assumptions.

Figure 2. Slide scanner image of a 7-μm thick foil from detector 3 of AVGR shot 011015 (a 248-gm sample of Northwest Africa 620, an unclassified ordinary chondrite), which was mounted 48 cm from the target, roughly 240° in azimuth from the direction of the incoming projectile The image resolution is 2700 dpi.

Preliminary Results: Analysis of the foil image data is still underway. Results presented here, however, are illustrative of the data sets that are being used to extend the SFDs of the fragments from the disruption of other meteorite samples down to dust-size particles.

Ideally, each target meteorite target would have been completely surrounded by foil, documenting the size frequency distribution of the dust-size fragments over the full 4π geometry. However, this in not practical, since the foil must be rigidly supported to minimize tearing from low-speed punctures. Further, it is not practical to count the penetrations in such a large area of foil. So, each of the foils was mounted in a 35mm slide mount, with an exposed area of 8.05 cm^2. In order to combine the scanner data from the individual foils, the area of each individual foil is normalized to its projected area on a virtual 1-meter radius sphere centered on the target. The ratio of the surface area of the virtual 1-meter radius sphere (125,664 cm^2) to the total projected area covered by all the foils for each shot is the correction factor used to scale the foil data to full 4π steradians. These data can now be compared with the mass-frequency distribution of the large fragments that were collected and weighed.

Figure 3 shows the resulting combined mass-frequency distribution for AVGR shot 020506 (a 105-gm sample of the meteorite Saratov). The foil penetration data (from all eight of the 7- and 13-μm thick foils deployed for this shot) are seen to nicely extend the mass data from the larger collected and weighed fragments (which were weighed to a completeness limit of ~0.02 gm). The nearly linear, power law-like mass-frequency distribution (with slope index approximately -0.99) displayed by the larger fragments extends nearly another two orders of magnitude in particle mass, until breaking to a shallower slope (with slope index approximately -0.22) for masses less than a few 10^{-4} gm.

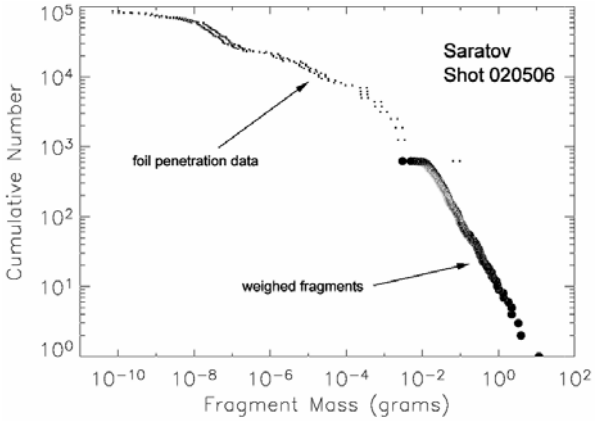

Figure 3. Combined mass-frequency distribution for fragments from AVGR shot 020605 (a 105-gm sample of the meteorite Saratov).

Similar data from the foils from 13 other shots involving chondritic meteorite targets are being combined to extend the mass frequency distributions of mm- to cm-scale fragments down to dust-size particles. The dust SFDs will provide very useful knowledge of the primary fragment SFDs to much smaller sizes than is conventionally measured in laboratory impact experiments.

References: [1] Durda D. D., Flynn G. J., Hart S. D., and Asphaug E. (2002) *LPS, XXXII*, abstract #1535. [2] Flynn G. J and Durda D. D. (2004) *Planet. Space Sci.*, **52**, 1129-1140. [3] Flynn G. J. et al. (1996) *LPS, XXVII*, 369. [4] Sandel L. E., M. M. Strait, D. D. Durda, and G. J. Flynn (2006) *LPS, XXXVII*. [5] Hörz F. et al. (1995) *NASA Technical Memorandum 104813*.